

The Outbursts of Dwarf Novae

M. R. Truss, J. R. Murray, G. A. Wynn and R.G. Edgar

Department of Physics and Astronomy, University of Leicester, University Road, Leicester, LE1 7RH, UK

31 October 2018

ABSTRACT

We present a numerical scheme for the evolution of an accretion disc through a dwarf nova outburst. We introduce a time-varying artificial viscosity into an existing smoothed particle hydrodynamics code optimised for two and three-dimensional simulations of accretion discs. The technique gives rise to coherent outbursts and can easily be adapted to include a complete treatment of thermodynamics. We apply a two-dimensional isothermal scheme to the system SS Cygni and present a wide range of observationally testable results.

Key words:

accretion, accretion discs - instabilities - hydrodynamics - methods: numerical - binaries:close - novae, cataclysmic variables.

1 INTRODUCTION

Dwarf novae are a class of cataclysmic variable which undergo regular but aperiodic phases lasting several days during which the system brightness increases by two to four magnitudes. These are the well known *normal outbursts* of dwarf novae, and they recur on time-scales of weeks to months. There is a well-known bimodal distribution of orbital periods of cataclysmic variables, with a dearth of systems having orbital periods in the range $2.2 \leq P_{\text{orb}} \leq 2.8$ hours. This is known as the period gap. Dwarf novae which lie above the period gap and only display normal outbursts are classified as U Geminorum systems, after their template. There is a roughly linear period-mass ratio relation for interacting binaries (Frank, King and Raine, 1995). The SU Ursae Majoris systems, which lie below the period gap and have more extreme mass ratios $q = \frac{M_2}{M_1} < 0.25$ show longer, slightly brighter superoutbursts lasting for ten days or more. These occur in addition to normal outbursts (typically one superoutburst occurs for every 5 to 15 normal outbursts) and show a superimposed periodic variation in brightness at supermaximum (superhumps). In this paper we introduce a numerical method for studying dwarf nova outbursts and apply it to a system of the U Gem class. In a future paper we will present the application to the SU UMa class (Truss et al, 2000).

Historically, two theories have been put forward to explain the outbursts of dwarf novae. Paczyński et al (1969) suggested that a low mass Roche-lobe-filling secondary is potentially unstable and mass transfer may occur quickly enough that its convective envelope would become radiative. The enhanced radiation subsequently stabilises the mass transfer and in this way an outburst cycle is initiated. How-

ever, observations of the hot-spot (the bright point at which material enters the disc) do not show an increase in brightness during outburst, as would be predicted by such a mass-transfer instability model (see for example, Rutten et al (1992)). The currently favoured model, and the model which we apply here, is that of an instability in the accretion disc itself. Integration of the density profile normal to the plane of the disc $\rho(z)$ yields a relationship between surface density Σ and temperature T (or mass-transfer rate) for an annulus in the disc. This is the well-known *S-curve* and is shown schematically in Figure 1. It represents the locus of points for which the annulus remains in thermal equilibrium. The physical basis which underpins the S-curve is the onset of hydrogen ionization. Hence the upper and lower branches of the curve correspond to the high and low opacity states of ionized and neutral hydrogen. The opacity function $\kappa(T)$ is very steep in the range 6000 - 7000 K; such an abrupt change leads to the instability. We can define the local viscous energy generation rate per unit area by

$$Q^+ = \int q^+(z) dz \quad (1)$$

where q^+ is the local viscous heat generation rate per unit area, assumed to be concentrated in the centre of the disc. Heat losses can be assumed to be from black-body dissipation from the disc surface. If the surface temperature is T_s , then the local energy dissipation rate is

$$Q^- = 2\sigma T_s^4, \quad (2)$$

where each surface of the disc contributes σT_s^4 . In thermal equilibrium, $Q^+(T_c) = Q^-(T_s)$, where T_c is the central disc temperature.

An annulus residing on the lower (quiescent) or upper

arXiv:astro-ph/0007186v1 13 Jul 2000

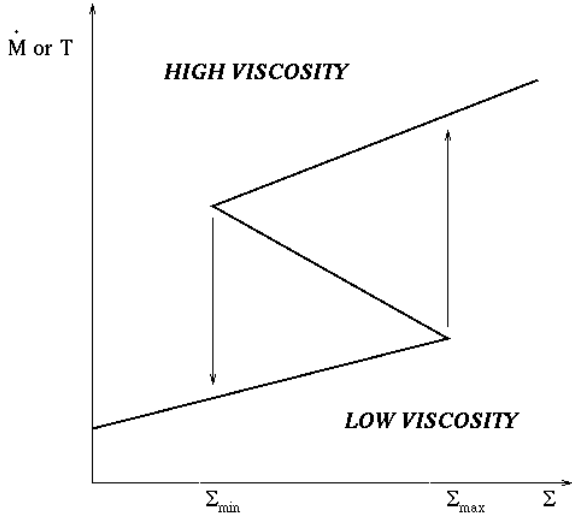


Figure 1. The limit-cycle behaviour of an accretion disc in a dwarf nova.

(outburst) branch of the curve subject to perturbations in local surface density can evolve on a viscous time-scale and remain in thermal equilibrium. No stable solution is available to an annulus in the middle branch, however. Here, if the mass-transfer rate (and hence T_c) is increased, Q^+ increases faster than Q^- and T_c rises yet further. Therefore, at the inflection points of the curve, the disc will evolve on a thermal time-scale (that is, very rapidly) to the opposite branch. In this way a limit cycle of quiescence and outburst is established. We interpret the upper and lower branches of the curve as high and low viscosity states. The critical surface densities at the points of inflection have been calculated by Cannizzo et al (1988) :

$$\Sigma_{\max} = 11.4 R_{10}^{1.05} M_1^{-0.35} \alpha_{\text{cold}}^{-0.86} \text{ g cm}^{-2} \quad (3)$$

$$\Sigma_{\min} = 8.25 R_{10}^{1.05} M_1^{-0.35} \alpha_{\text{hot}}^{-0.8} \text{ g cm}^{-2} \quad (4)$$

where R_{10} is the radius in units of 10^{10} cm, M_1 is the mass of the primary in solar masses and α_{hot} and α_{cold} are the Shakura-Sunyaev viscosity parameters in the high and low states. Note that these are very close to linear radial dependences. An excellent review of the dwarf nova disc instability is given by Cannizzo (1993a).

We begin with a full explanation of our model and the numerical techniques involved in applying a smoothed particle hydrodynamics (SPH) approach to the problem. In Section 3 we demonstrate that our model is physically consistent with a real dwarf nova and present a wide range of simulated observables.

2 MODELLING DWARF NOVA OUTBURSTS

2.1 The Smooth Particle Hydrodynamics Technique

In this section we discuss substantial developments made to an existing smooth particle hydrodynamics accretion disc code that enable us to model the complete outburst cycle of a dwarf nova. The principal change is the modification

of the dissipation term to make it a function of local disc conditions. Smooth particle hydrodynamics (SPH) is a Lagrangian method for modelling the dynamics of fluids. A continuous medium is modelled by a collection of particles that each move with the local fluid velocity. Fluid properties at any given point are determined by interpolating from the particle positions. The interpolation takes the form of a simple summation over the particles with each term weighted according to distance from the point in question. The weighting function is known as the interpolation kernel. For example, the interpolated value for the density at some point \mathbf{r} in the fluid

$$\rho(\mathbf{r}) = \sum_i^n m_i W(\mathbf{r} - \mathbf{r}_i, h), \quad (5)$$

where the sum is over all the particles. Here, m_i and \mathbf{r} are the mass and position of particle i respectively. W is the interpolation kernel which has a characteristic length-scale h , commonly called the smoothing length. For a general introduction to SPH the reader is referred to Monaghan (1992).

In Murray (1996) an SPH code specifically modified for accretion disc problems was described. The key feature of this code was the use of an artificial viscosity term in the SPH equations to represent the shear viscosity ν known to be present in observed discs. The artificial viscosity term introduces, in the continuum limit, a fixed combination of shear and bulk viscosities to the fluid. The viscous force per unit mass,

$$\mathbf{a}_\nu = \kappa \zeta c L (\nabla^2 \mathbf{v} + 2\nabla(\nabla \cdot \mathbf{v})). \quad (6)$$

κ is an analytically determined constant that depends upon the kernel. $\kappa = 1/8$ and $1/10$ for the cubic spline kernel in two and three dimensions respectively. c is the sound speed, \mathbf{v} is the fluid velocity and L a viscous length scale. In previous work L was taken to be equal to the smoothing length h . Here however we relax that constraint. ζ is a dimensionless parameter. Note that in most SPH papers this parameter is denoted α but we have followed Murray (1996) and renamed it to avoid a confusion of subscripts.

In the interior of Keplerian discs we can neglect the velocity divergence and we see that the artificial viscosity term generates a shear viscosity

$$\nu = \kappa \zeta c L. \quad (7)$$

We can control the shear viscosity throughout the disc by modifying ζ and L , and so obtain a functional form very similar to the Shakura-Sunyaev form used in accretion disc theory.

Several tests of this code were presented in Murray (1996). The code has been used to look at tidally unstable discs (Murray 1998, 2000), tilted discs (Murray & Armitage 1998) and counter-rotating discs (Murray, deKool & Li, 1999) around accreting pulsars. Kornet & Różycka (2000), using an Eulerian code (quite distinct algorithmically from the SPH code we use), have reproduced several of the results of Murray (1998).

2.2 Outbursts

As mentioned in the previous section, quiescence is associated with a very low value of the Shakura-Sunyaev shear

viscosity parameter (α) but also a low temperature. In outburst, angular momentum transport is much more rapid because the temperature is much higher and α is much larger. In previous papers (Murray 1998, Armitage & Murray 1998) preliminary attempts were made to model outbursts by instantaneously increasing the value of the shear viscosity throughout the entire disc. Such an approach only enabled us to model the most basic features of an outburst, and we could not of course follow the propagation of state changes through the disc. The principal modification to the code made for this work was to allow the viscosity to change locally in response to disc conditions. This was easy to do, simply requiring that each particle carry a variable ζ that determined its 'viscosity'. To determine the viscosity of the interaction of any particular pair of particles we use the harmonic mean of the two ζ values. Cleary & Monaghan (1999) found that such a form gave good results for heat conduction between materials with vastly different properties.

All that remained was to determine how changes in viscosity were to be triggered. The simplest approach is to let the shear viscosity of each SPH particle be determined by the local surface density Σ . If, for some region of the disc in the quiescent state, the surface density is less than some critical value Σ_c that region of the disc is assumed to be stably quiescent, and the particle's shear viscosity remains at a value appropriate for a cool disc. Should Σ increase to be greater than Σ_c then we consider that region of the disc to have been 'triggered' into the hot state. We then let the particle's shear viscosity increase to a value appropriate for a hot disc (the details of the transition are described below). The viscosity continues adjusting to its new value even if Σ subsequently drops below Σ_c . Conversely a hot region of the disc is stable as long as its surface density remains above a second critical value $\Sigma_h < \Sigma_c$. However if a portion of the disc has $\Sigma < \Sigma_h$ then that particle's shear viscosity parameter will reduce to the quiescent value (See figure 2). Σ_h and Σ_c correspond to Σ_{\min} and Σ_{\max} . We preserve their radial dependence but reduce the magnitude of their gradients to reduce the run-time of the code. A full analysis of the scaling is given in Section 3.2.

In previous work (Murray 1998, Armitage & Murray 1998) α was set to change instantaneously between quiescent to outburst values. In this work, we assume that when the instability is triggered, the viscosity changes on the thermal time scale. As we have limited knowledge of the mechanism responsible for accretion discs' high viscosity, we can only propose an appropriate functional form for the transition. We use the hyperbolic tangent function as it allows us to capture both the initial exponential change in ν and a smooth asymptotic approach to its final value. In terms of the Shakura-Sunyaev viscosity parameter, the equation for the transition from quiescence ($\alpha = \alpha_{\text{cold}}$) to outburst ($\alpha = \alpha_{\text{hot}}$) is

$$\alpha(t) = \frac{(\alpha_{\text{hot}} + \alpha_{\text{cold}})}{2} + \frac{(\alpha_{\text{hot}} - \alpha_{\text{cold}})}{2} \tanh\left(\frac{t}{t_{\text{th}}} - \pi\right) \quad (8)$$

and the converse, for the transition from α_{hot} to α_{cold} is

$$\alpha(t) = \frac{(\alpha_{\text{hot}} + \alpha_{\text{cold}})}{2} - \frac{(\alpha_{\text{hot}} - \alpha_{\text{cold}})}{2} \tanh\left(\frac{t}{t_{\text{th}}} - \pi\right). \quad (9)$$

The functional form of the trigger is shown in Figure 3. Of course, \tanh doesn't have compact support, so as soon

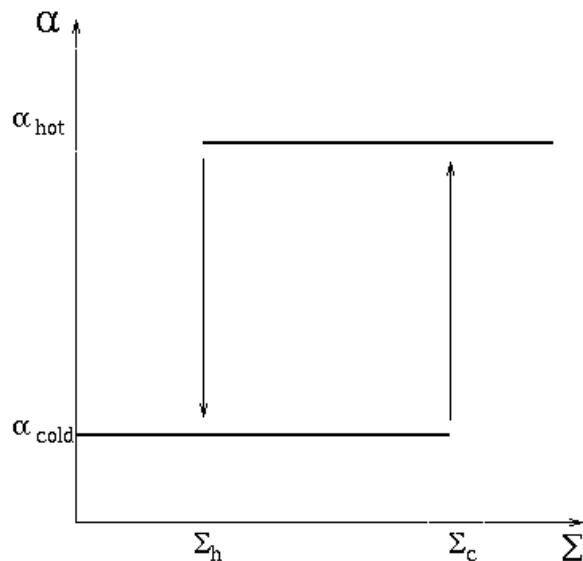


Figure 2. The simplified surface density trigger conditions used in the code. Σ_c and Σ_h are functions of radius in the disc.

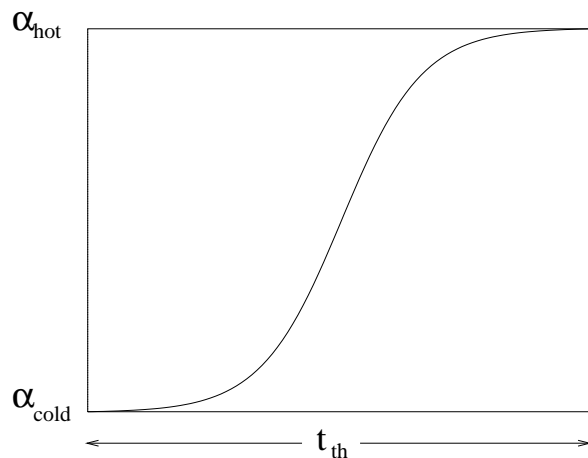


Figure 3. Functional form of the outburst trigger. The viscosity is switched on a total time-scale t_{th} .

as a transition has been triggered we add a small artificial offset to α .

In the following section we describe simulations completed with the new variable viscosity. As well as using a density trigger in which single SPH particles could change state, we implemented a more coarse grained approach. The disc was divided into a set of concentric annuli (typically 100 were used). When the mean surface density in a given annulus met the triggering conditions, then all particles in that annulus changed state (again on the thermal time scale). This intermediate, azimuthally smoothed, approach improved the speed of the code by $\sim 50\%$, and provides a suitable basis for incorporation of a full thermodynamic treatment of the thermal instability. The calculations described in the next section demonstrate that these two approaches to the viscosity switching are consistent with one another.

As it is written, the triggering routine can simply be re-

placed by a more thermodynamically sophisticated routine. Preliminary calculations have indeed been made. However, as these simulations are proving more computationally demanding, we leave them to a later paper.

3 RESULTS

We show that our fast azimuthally-smoothed approximation gives a good representation of the physical behaviour of the system and move on to present a wide range of results and analysis for a simulation of the dwarf nova SS Cygni. SS Cygni is a very well-observed dwarf nova of the U Gem type. It has an orbital period of 0.275130 days and a mass ratio (defined as mass of the mass-losing secondary to that of the accreting white dwarf primary) of 0.59 ± 0.02 , with $M_1 = 1.19 \pm 0.02 M_\odot$ (Friend et al, 1990).

All the results presented in this paper are for *steady state* discs, which we define to be those which return to the same quiescent level between outbursts. We take a constant mass-transfer rate of $10^{-9} M_\odot \text{yr}^{-1}$ throughout the simulations, following Cannizzo (1993b).

3.1 Comparison of triggering regimes

The simulation was performed with both local triggering and azimuthally smoothed triggering as detailed above. In the case of local triggering, two regimes are contrasted; (i) $\tau_{\text{trigger}} = 250$ s, (ii) $\tau_{\text{trigger}} = 5000$ s. For the azimuthally smoothed case, we choose a long trigger timescale of 7500 s. The thermal time-scale t_{th} and the dynamical (Kepler) time-scale t_ϕ are related by

$$t_\phi \sim \alpha t_{\text{th}}, \quad (10)$$

SS Cygni has an orbital period of almost 400 minutes and a Kepler timescale of around 250 seconds at the circularisation radius. This is the radius at which the gas has the same specific angular momentum as it had on passing through the L_1 point (i.e. as it is injected into the model). It is the radius at which infalling gas would first orbit the primary before formation of an accretion disc. Hence for realistic values of α ($\ll 1.0$), t_{th} will be of the order of a few thousand seconds, which we use in the azimuthally smoothed code and case(ii).

Figure 4 contains plots of total viscous dissipation against time for the different regimes. The outbursts in both cases are coherent, that is a large region of the disc is transformed to the hot state. It is clear that the azimuthally smoothed result is consistent with a local trigger time-scale somewhere between these two cases. The peak-to-peak time-scale between outbursts is around 30 days in the smoothed code, 20 days in the shorter timescale code and 40 days in the longer time-scale code. Our fast azimuthally smoothed code is consistent with the physically realistic case of a thermal time-scale greater than the Kepler time-scale.

3.2 Light curves

Figure 5 shows light curves calculated from the SS Cygni simulation in the U,B,V,J,H and K bands. These are calculated by assuming that the disc is optically thick and each annulus of gas in the disc radiates as a black body. We then

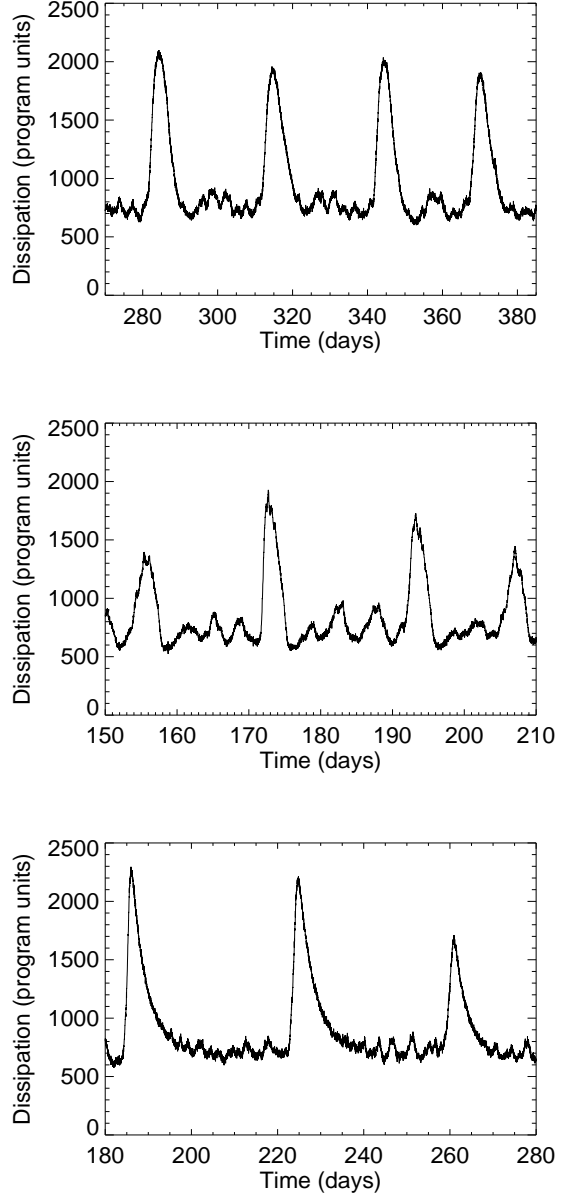


Figure 4. Top : Light curve (total viscous dissipation) in SS Cygni simulation with azimuthal smoothing and $\tau_{\text{trigger}} = 7500$ s. Middle : Light curve with local triggering and $\tau_{\text{trigger}} = 250$ s. Bottom : Light curve with local triggering and $\tau_{\text{trigger}} = 5000$ s

simply integrate the Planck function over different wavebands and sum over the annuli to yield the light curves.

The light curves show regular normal outbursts with a comparatively rapid rise to maximum and a slightly longer fall to quiescence. The amplitude of the normal outbursts in the V band varies around 1.5 magnitudes on our diagram, with a rise-time of ~ 2.5 days and a decay-time of ~ 4.5 days. SS Cygni is observed to brighten from 12th magnitude in quiescence to 8th magnitude in outburst. Our result is suppressed by the artificially high value of the Shakura-Sunyaev alpha parameter in the two states, which we use to reduce the run-time of the code. We can make an estimate of the compression factor of the amplitude as follows. The

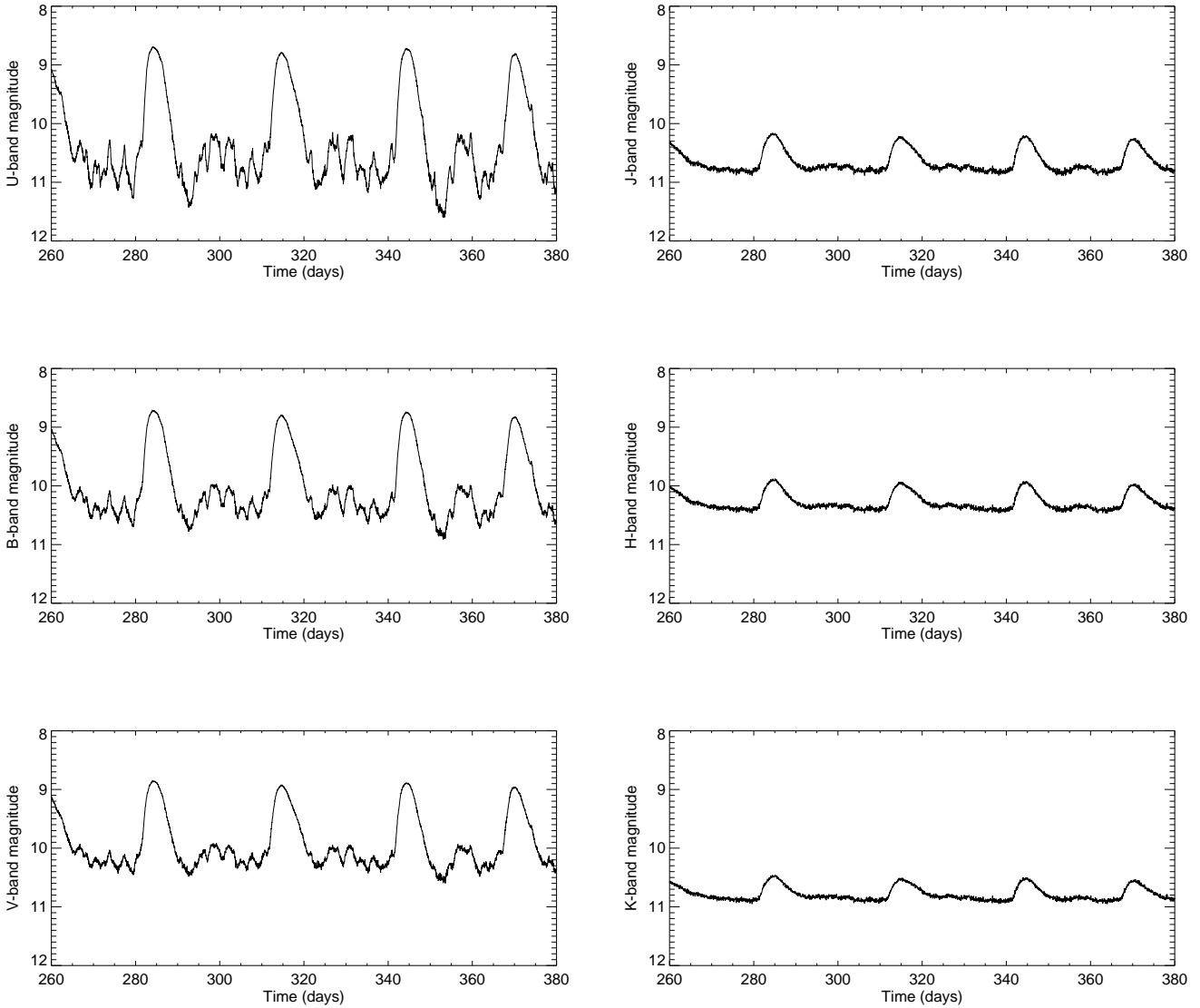


Figure 5. U,B,V,J,H and K filter band light curves (azimuthally-smoothed model). The light curves show three distinct states - outburst, quiescence and minioutbursts

dissipation rate of an accretion disc $D(R)$ is directly proportional to the torque exerted by one annulus on another $G(R)$:

$$D(R) = \frac{G(R)}{4\pi R} \frac{d\Omega}{dR} \quad (11)$$

where Ω is the angular velocity of the gas in the annulus. The viscous torque is

$$G(R) = 2\pi R \nu \Sigma R^2 \frac{d\Omega}{dR} \quad (12)$$

where ν is the viscosity, so

$$D(R) = \frac{1}{2} \nu \Sigma \left(R \frac{d\Omega}{dR} \right)^2 \quad (13)$$

The dissipation rate is therefore proportional to $\nu \Sigma$. Equation 7 gives the relationship between ν and the alpha-

parameter (ζ in Eq.7). In an isothermal disc, the ratio of total dissipation in outburst to that in quiescence is

$$\frac{D_{\text{outburst}}}{D_{\text{quiescence}}} = \frac{(\alpha \Sigma)_{\text{outburst}}}{(\alpha \Sigma)_{\text{quiescence}}} \quad (14)$$

We use a simple 1:10 ratio of α irrespective of surface density Σ . The density triggers are set at

$$\Sigma_{\text{max}} = 16.67 \frac{R}{a} \text{ gcm}^{-2} \quad (15)$$

$$\Sigma_{\text{min}} = 6.250 \frac{R}{a} \text{ gcm}^{-2} \quad (16)$$

where a is the binary separation. The surface density at the peak of outburst will be close to Σ_{min} , while the surface density in quiescence just before an outburst will be close to Σ_{max} . This is clearly shown in Fig. 9. Therefore, in our isothermal disc simulation,

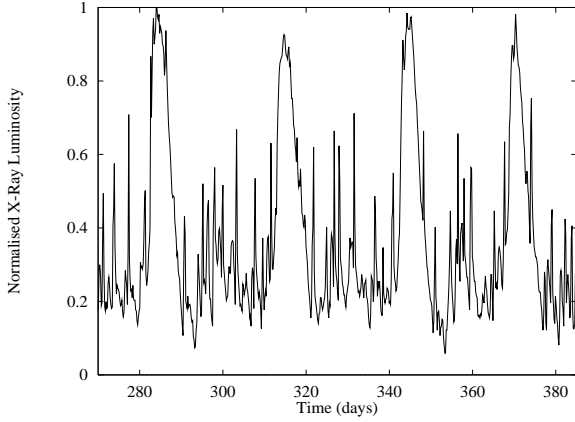


Figure 6. Top : X-ray light curve generated from number of simulation particles accreted onto the primary.

$$\frac{D_{\text{outburst}}}{D_{\text{quiescence}}} = \frac{\alpha_{\text{hot}} \Sigma_{\text{min}}}{\alpha_{\text{cold}} \Sigma_{\text{max}}} \simeq 3.7. \quad (17)$$

Real discs, however, are not isothermal. Rewriting Eq.7 in terms of more familiar quantities for a thin Shakura-Sunyaev disc,

$$\nu = \alpha c_s H \sim \alpha c_s^2 \left(\frac{R^3}{GM} \right)^{1/2} \quad (18)$$

where c_s is the sound speed and H is the scale height. In the limit where we can neglect radiation pressure,

$$c_s^2 = \frac{P}{\rho} \propto T_c \quad (19)$$

where T_c is the midplane temperature. The critical surface densities will be given by (3) and (4) and in a real disc at fixed radius,

$$\frac{D_{\text{outburst}}}{D_{\text{quiescence}}} = \frac{8.25 \alpha_{\text{hot}} T_{c,\text{hot}} \alpha_{\text{hot}}^{-0.8}}{11.4 \alpha_{\text{cold}} T_{c,\text{cold}} \alpha_{\text{cold}}^{-0.86}} \quad (20)$$

Using Cannizzo's (1993b) values of $T_{c,\text{hot}} \simeq 60,000\text{K}$ and $T_{c,\text{cold}} \simeq 4,000\text{K}$, and setting $\alpha_{\text{cold}}=0.01$ and $\alpha_{\text{hot}}=0.1$, this ratio is about 13.1. The compression factor introduced in dissipation amplitude by the code is about 3.5, bringing our result closer to the equivalent observed amplitude in SS Cygni.

In the quiescent phase, there appears to be an additional modulation in luminosity. These aperiodic *minioutbursts* appear in clusters and are particularly blue, suggesting that only the hot inner portion of the disc is involved in producing the additional luminosity. These variations are indeed observed in the V-band light curve of SS Cygni (see, for example, the AAVSO light curves).

It is possible to correlate the number of particles being accreted onto the white dwarf primary with an expected X-ray luminosity for the system by simple consideration of gravitational energy released. For simulation particles of mass M_p , the X-ray luminosity produced is

$$L_X = \epsilon \frac{GM_p}{R} \frac{dM}{dt} \quad (21)$$

where ϵ is an unknown efficiency factor expected to be $\ll 1$. An X-ray light curve can be built up in this way and is presented in Figure 6 for our simulation. In quiescence and on the decline from outburst, the X-ray emission follows the

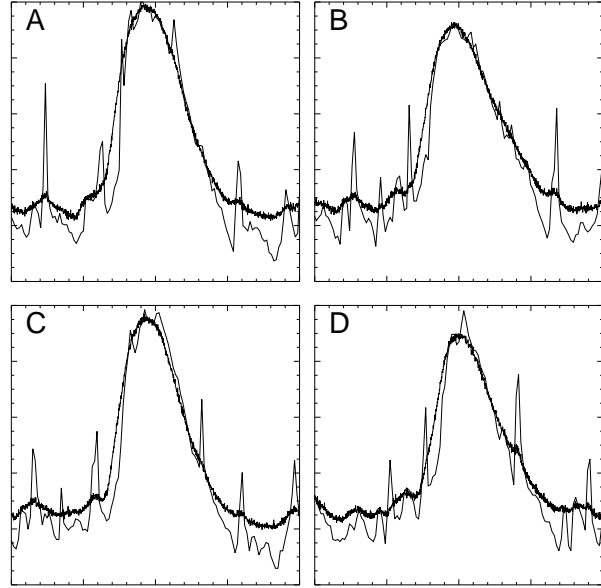


Figure 7. Overlay of V-band (dark line) and X-ray emission for the four outbursts in Figure 5. Each plot has been normalised to the peak of curve A and shows a 20-day time series.

optical emission very closely; indeed our X-rays appear to be very sensitive to fluctuations in the V-band in quiescence. However, there is a noticeable and significant delay in the onset of the outbursts. This is shown in Figure 7 for each of the four outbursts. Each plot shows 20 days; referring back to Figure 5 we have A : 275-295 days, B : 305-325 days, C : 335-355 and D : 360-380 days. The optical rise leads the X-ray rise by up to a day in all our outbursts. This can be interpreted as the time required for the gas in the part of the disc which initially goes into outburst to migrate through the inner disc before it is accreted onto the primary. The measurement of the delay is in good agreement with observation; Jones & Watson (1992) found a typical delay of 0.5 - 1.1 days from EXOSAT observations. The rise-time is also seen to be much faster in X-rays; we find a rise-time of ~ 12 hours in X-ray and ~ 2.5 days in the optical. The climb in V-band emission is a gradual process as more and more gas in the disc is transformed to the high state, whereas the onset of enhanced accretion onto the white dwarf itself is instantaneous, triggered when the additional material from the outbursting disc arrives at its surface.

3.3 Disc Analysis

In this section we follow the evolution of an accretion disc through an outburst cycle. The light curves give much information about the physical processes taking place in the disc during quiescence and outburst, but a much clearer representation is obtained by following the dynamical behaviour of the accretion disc itself. Figure 8 is a montage of images of the accretion disc through a normal outburst. We find that even in quiescence ($t=334.2$), a small fraction of the inner disc remains permanently locked in the hot state. The linear relation between the critical surface density triggers and the disc radius ensures that particles in the inner disc are continually cycling between the low and high states (the

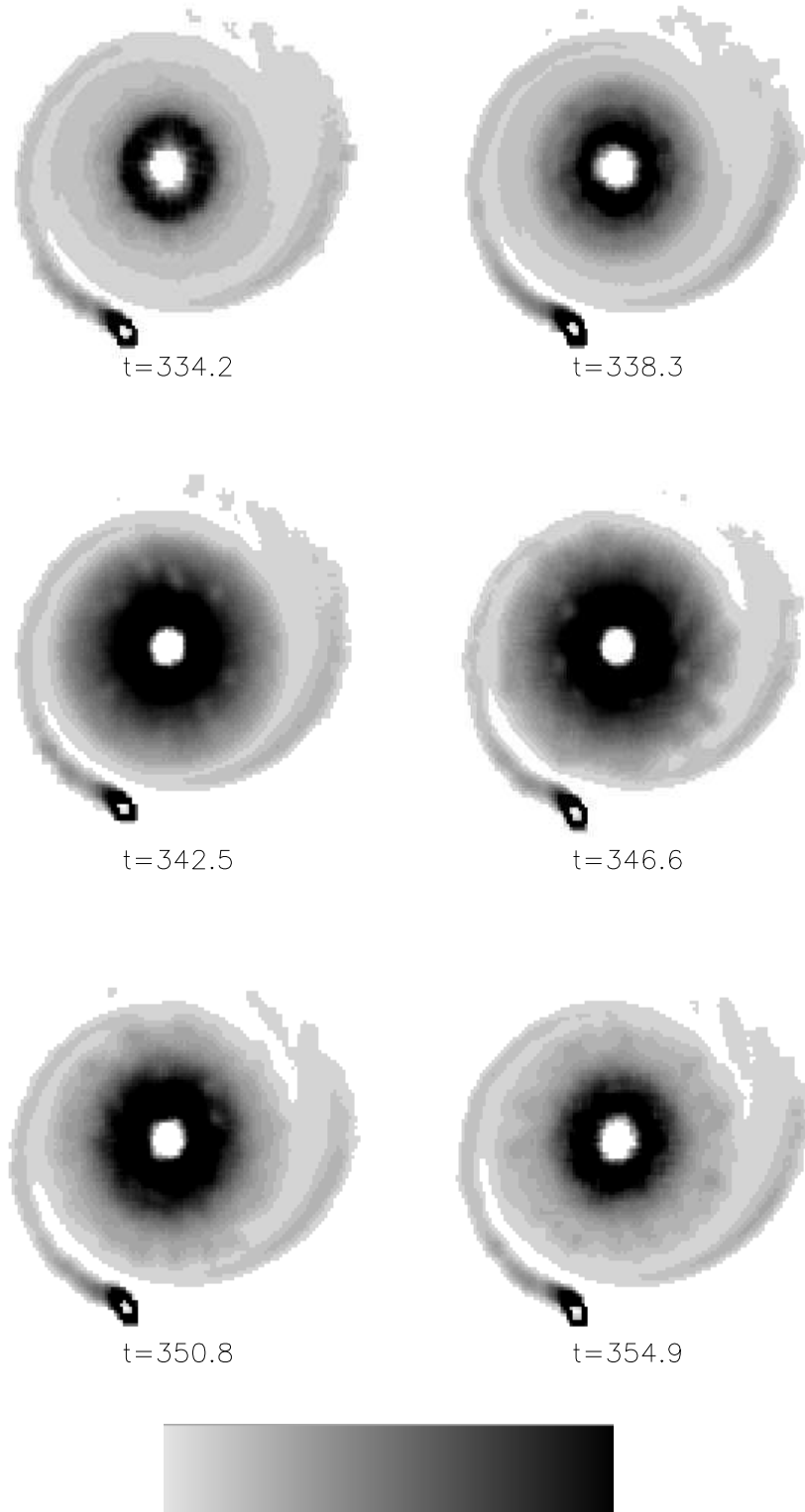


Figure 8. Evolution of total viscous dissipation in the disc through an outburst. The greyscale is logarithmic with white at $10^7 \text{ ergs}^{-1} \text{ cm}^{-2}$ through to black at $10^9 \text{ ergs}^{-1} \text{ cm}^{-2}$. The discs are aligned such that the primary-secondary axis is vertical and the hot-spot appears at the bottom of each frame. Spiral shock arms are also clearly evident. t is the time in days. Note that the central part of the disc (white) is not modelled in the simulation.

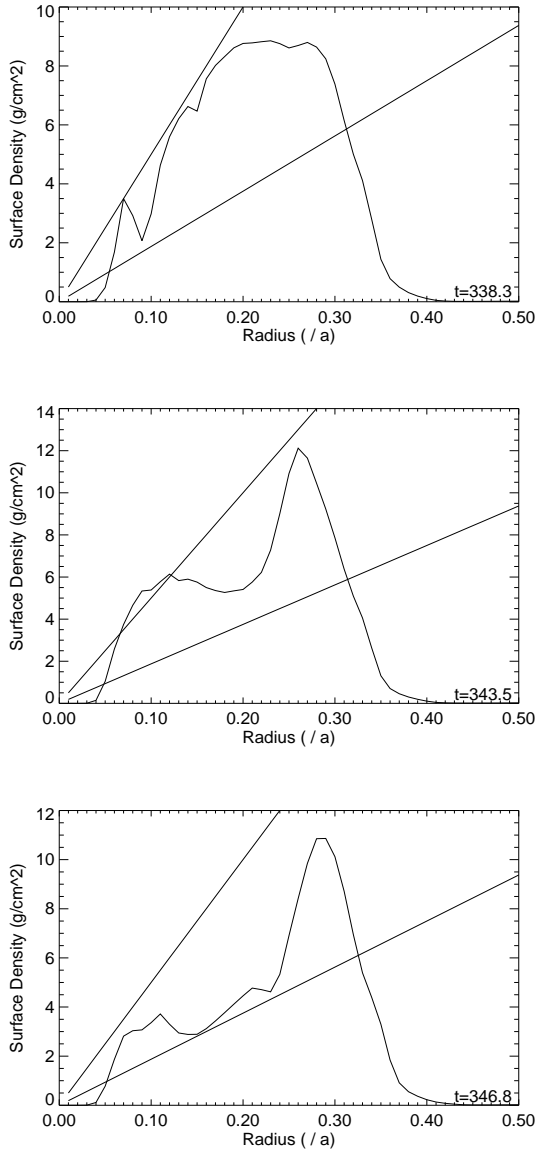


Figure 9. Evolution of azimuthally-averaged surface density of the disc through an outburst. The straight lines show the radial dependence of the upper and lower triggers. a is the binary separation, 1.8×10^{11} cm in SS Cyg.

triggers are very close together here and also very low - these conditions are easily satisfied by particles close to the primary). The rise to outburst is rapid and is initiated in the inner part of the disc. A density wave (directly analogous to a heating wave in a full thermodynamic treatment) moves both outwards and inwards, transforming a large fraction of the disc to the hot, high viscosity state. Subsequently the disc falls (less rapidly) back into quiescence by another density wave (analogous to a cooling wave). This pattern is repeated for all the normal outbursts. Approximately the same fraction of the disc is seen to reach the high state in each outburst. The maximum extent of the hot portion is seen to vary to a small degree, but appears ultimately to be limited to a radius near the position of the spiral shock arms. This can be readily observed in the light curve - some



Figure 10. The disc in minioutburst. The outburst has not propagated far enough to become a normal outburst. The greyscale is the same as in Fig. 8.

outbursts reach a slightly higher peak luminosity than others, although the maximum variation is no more than a few percent.

The outburst is, of course, triggered by the local surface density in the disc and as the gas in the disc is accreted inwards on a viscous timescale there is a corresponding change in that local surface density. This response is shown in Figure 9. The disc clearly drains during the outburst phase until the local surface density reaches the lower trigger level, after which the outburst dies away and the disc is replenished. These density profiles are extremely similar to those found by Stehle (1999) in a full thermodynamic one-dimensional treatment (not SPH).

Figure 10 shows a disc in minioutburst, and confirms our observation from the light curve in section 3.2 that it is the inner disk which is hot in a minioutburst. The outburst is initiated very near the inner edge of the disc and never propagates very far. The reason for this can be seen in Figure 9. Just before a normal outburst (top panel), the surface density profile follows the line of the upper trigger very closely. Any part of the disc that goes into outburst will lead to a coherent normal outburst throughout most of the disc. After a normal outburst (bottom panel), the only part of the disc near the upper trigger is near the disc centre. All the remainder of the disc has been drained. Hence while the centre of the disc can go into outburst, the majority of the disc cannot. This is what happens in a minioutburst.

Disc spectra, temperature profiles and luminosity profiles clearly show the contrast in the physical properties of the disc in the different states. The spectra, in Figure 11, have been computed for the disc in outburst, quiescence and minioutburst. The blue, hot inner disk behaviour in minioutburst becomes clear in comparison with the quiescent spectrum.

The luminosity and temperature profiles in Figure 12 have been calculated on the rise to a normal outburst, and

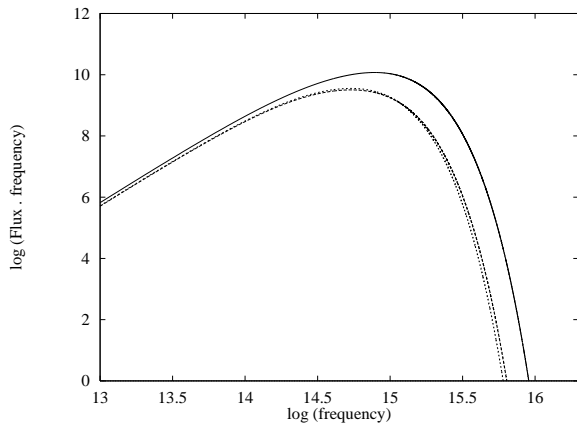


Figure 11. Disc spectra in quiescence (bottom curve), minioutburst (middle) and outburst (top). The disc in minioutburst is bluer than the quiescent disc.

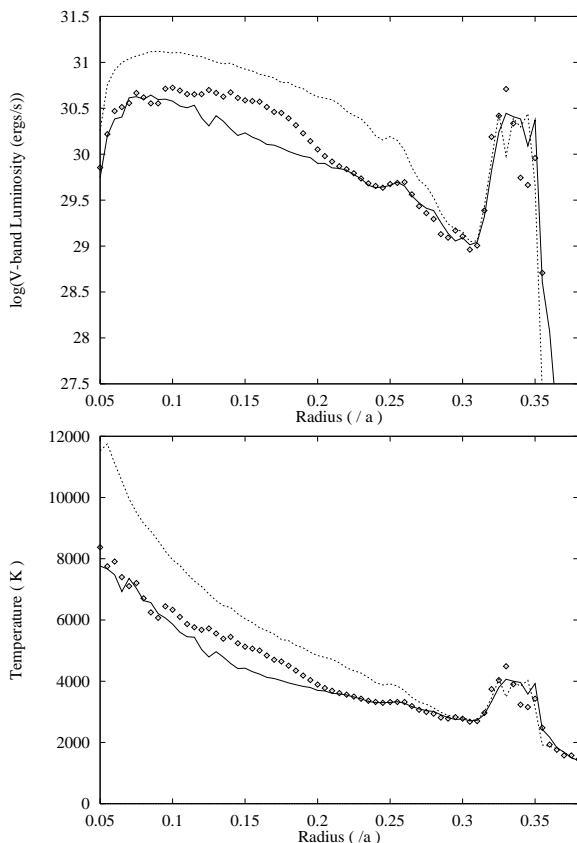


Figure 12. V-band luminosity and temperature of the disc evolving through the rise to normal outburst. The inner region of the disc remains in outburst even during quiescence (solid line) and the normal outburst is initiated at a radius around $0.15a$ (points). The dashed line represents the profile at peak outburst.

correspond to the discs in the first three frames of Figure 8. All the profiles show an increased region of viscous dissipation (and temperature) near the outer edge of the disk, where the surface density peaks as matter enters the disc from the accretion stream; this is the *hot-spot*. This normal outburst is apparently triggered at a radius of approximately $0.15a$ (near the circularisation radius - $0.11a$ in SS

Cyg) and the heating wave is seen to propagate in both directions. We find that in quiescence the disc is typically approximately isothermal at radii greater than $0.15a$ at temperatures around 4000 K. In outburst we find temperatures ranging from 6000 K to 12000 K in the inner half of the disc and 4000 K to 6000 K in the outer half. Bobinger et al (1997) have performed eclipse mapping of the dwarf nova IP Peg, which has strikingly similar parameters to SS Cyg ($q = 0.58$, $P = 0.158d$), on the decline from outburst. They found an inner disc at 7000 K to 9000 K and an outer disc with temperatures declining to a quiescent level of 3000 K to 4000 K. Our simulated results are in good agreement with these observations. Figure 12 also shows that the hot-spot is consistently around 1500 K hotter than the surrounding regions, but the increase in luminosity from these regions is much more marked - the viscous dissipation is 30 times higher here than in the part of the disk just inside them. The accretion rate from the secondary is constant in this simulation, so we find a constant hot-spot temperature. It is also interesting to note, however, that the luminosity generated in the hot-spot of the quiescent disc is comparable to that generated by the very hot inner part of the disc.

4 DISCUSSION

We have performed the first two-dimensional treatment of dwarf nova outbursts. The method gives light curves in different wavelength bands, disc spectra, density and temperature profiles which all agree well with observations and full thermodynamic analyses.

The advantages of using a two-dimensional code to model dwarf nova outbursts are immediately obvious. Tidal forces are not approximated as in one dimensional codes and therefore much more detail is revealed in the results of these current simulations. One dimensional simulations have always predicted extremely regular outburst behaviour, both in recurrence pattern and outburst profile. There is now much more scope for exploring the behaviour of these systems; the simulated observational characteristics presented here are just a selection of the possible areas which can be explored in future work.

We have applied these methods successfully to a study of the SU Ursae Majoris systems (Truss et al, 2000) in addition to the dwarf novae with less extreme mass ratios considered here. A two-dimensional code is ideal for exploring tidal effects and instabilities in such systems.

Observations of dwarf novae are by no means comprehensive or continuous, but this situation should be remedied in the near future with more telescope time dedicated to them. In consequence, it will be possible to test several of the results in this paper. Although our knowledge of the behaviour of dwarf novae in the V-band is good thanks to the efforts of organisations such as the AAVSO, there is little data available in other bands, so new observations will be able to probe the inner regions of the disc and (via X-ray observations) boundary layer. Our findings relating to a hot inner disc and the occurrence of minioutbursts should have some testable observational consequences.

The next stage of development of any numerical model such as this should be twofold : the incorporation of full thermodynamics into the simulation and the extension to

three dimensions. This is not a difficult task with the present scheme, just a lengthy one in computational terms. The increasing availability of parallel machines and improvements in CPU performance should make these refinements a workable proposition.

ACKNOWLEDGMENTS

Research in theoretical astrophysics at the University of Leicester is supported by a PPARC rolling grant. Many of the calculations were performed using GRAND, a high performance computing facility funded by PPARC and based at the University of Leicester. The authors are grateful to Dr R. Stehle, Prof. J. Pringle, Prof. A. King and an anonymous referee for helpful discussions or comments. MRT acknowledges a PPARC research studentship and a William Edwards Charitable Trust bursary for postgraduate study.

REFERENCES

- Armitage, P.J., Murray, J.R., 1998, *MNRAS*, 297, L81
 Bobinger A., Horne K., Mantel K., Wolf S., *A&A*, 327, 1023
 Cannizzo J.K., Shafter A.W., Wheeler J.C., 1988, *ApJ*, 333, 227
 Cannizzo J.K., 1993a, in *Accretion Disks in Compact Stellar Systems*, ed. Wheeler J.C.. World Sci.Publ.Co., Singapore
 Cannizzo J.K., 1993b, *ApJ*, 419, 318
 Cleary, P.W., Monaghan, J.J., 1999, *JCompPhys*, 148, 227
 Frank J., King A., Raine D., *Accretion Power in Astrophysics*, Cambridge University Press, 1995
 Friend M.T., Martin J.S., Connon-Smith R., Jones D.H.P., 1990, *MNRAS*, 246, 654
 Jones M.H., Watson M.G., 1992, *MNRAS*, 257, 633
 Kornet K., Różycka M., 2000, *astro-ph/003169*
 Monaghan J.J., 1992, *ARA&A*, 30, 543
 Murray J.R., 1996, *MNRAS*, 279, 402
 Murray J.R., 1998, *MNRAS*, 297, 323
 Murray J.R., 2000, *MNRAS*, in press
 Murray J.R., de Kool M., Li J., 1999, *ApJ*, 515, 738
 Paczyński B., Ziolkowski J., Zytkow A., 1969, in *Mass Loss from Stars*, ed. Hack M., Reidel, Dordrecht
 Rutten R.G.M., Kuulkers E., Vogt N., van Paradijs J., 1992, *A&A*, 265, 159
 Shakura N.I., Sunyaev R.A., 1973, *A&A*, 24, 337
 Stehle R., 1999, *MNRAS*, 304, 687
 Truss M.R., Murray J.R., Wynn G.A., 2000, in preparation